

ASPECTS OF REPAIR TECHNOLOGY OPTIMIZATION THROUGH NUMERICAL/EXPERIMENTAL MODELING

Ștefan F. Soroșan*, Nicolae S. Constantin*, Viorel I. Anghel*, Mircea C. Găvan*
*University "Politehnica" of Bucharest, Romania, naec@form.resist.pub.ro

Keywords: aeronautical aluminum structures, composite patches, bonding interface

Abstract

Repair of aeronautical aluminum structures is a good market, creating both economic and scientific challenges for technology providers and customers. The main targets of this technology consist in getting a repaired structure with a mechanical performance close to the original one, using a versatile technology and make it with minimum cost. The bonded composite patches seem to be a good solution for meeting all these demands, but research concerning details of the mechanical behavior of different variants, considering all the geometric and material parameters are still needed.

The paper presents extensive numerical results obtained in the study of aluminum/composite bonded joints, with optimized solutions based on the sensitivity of the mechanical behavior concerning geometric parameters, such as the thickness ratio and overlapping distance between bonded members, adhesive layer thickness and mechanical characteristics. The results are partly confirmed by experiments.

1 Introduction

The damaged aluminum aeronautical structures are generally repaired with aluminum patches applied with riveted or bolted joints to the main non-damaged elements. This technology is time consuming and can even create premises for further damage. For these reasons, repair technology using composite patches was proposed already 30 years ago [1], [2]. In spite of such quite long tradition, repair of aluminum aeronautical structures with composites is still looking for solutions conferring optimum structural behavior.

Atre and Johnson [3] presented the influence of riveting process parameters upon the strength of the aircraft fuselage lap joints showing that the effects of holes are dominant upon the cracks generation.

Caliskan [5] shows that the bonded repair is better than the bolted ones for repairing of composite single lap joints.

Recent research has shown that bonded joints strength is depending upon a lot of parameters, apparently non-essential in this kind of joints. For example, considering a bonded single lap joint between steel and FRP, Belingardi et al. [4] have analyzed in detail the effect of spew and chamfer size on the stress distribution in adhesive joints showing that for spew and chamfer angles of about 45° the peak stresses are considerably reduced.

Kelly [6] shows that hybrid joining offer potential improvement in strength and fatigue life in comparison to adhesive bonded joints.

In the research performed and presented in this work, behavior of bonded composite patches is mainly considered, as this solution seems to offer advantages the hybrid bonded/riveted one. The effectiveness of 2D and 3D FE modeling and the sensitivity analysis of bonding interface parameters, such as the glue thickness and stiffness, overlapping distance, thicknesses and stiffness of the composite patch are in view for getting optimized repair parameters. Comparisons with the hybrid bonded/riveted solution and experimental data are presented in support of the proposed repair technology.

2 Numerical Modeling

2.1 Assessment of 2D and 3D models

The bonding of a composite patch on a metallic panel was assessed by first modeling a sample made of aluminum sheet with $t_{Al} = 2 \text{ mm}$ thick, bonded with an equally thick $[0^\circ/90^\circ/0^\circ/90^\circ]_s$ carbon/epoxy laminate having a total thickness $t_c = 2 \text{ mm}$, all forming a $L_{tot} = 150 \text{ mm}$ long and $B = 25 \text{ mm}$ wide sample, with $L_a = 25 \text{ mm}$ overlapping distance and $t_a = 0.25 \text{ mm}$ thick glue was studied with a 2D FE model in plane strain condition (Fig. 1). For

aluminium, the constants of materials considered were: Young's modulus $E_{Al} = 73.1 \text{ GPa}$ and Poisson ratio $\nu_{Al} = 0.33$. For an orthotropic layer of the composite plate, the engineering constants are presented in the Table 1 and the adhesive was considered isotropic with $E_{Ad} = 1.25 \text{ GPa}$ and $\nu_{Ad} = 0.38$.

Table 1. Engineering constants of the composite plate

Young modulus [GPa]	Poisson ratio (major)	Shear modulus [GPa]
$E_1=98$	$\nu_{12}=0.34$	$G_{12}=4.7$
$E_2=7.8$	$\nu_{23}=0.44$	$G_{23}=3.2$
$E_3=7.8$	$\nu_{13}=0.34$	$G_{13}=4.7$

The spews and the chamfers in the adhesive joint were neglected.

The mesh was adaptive performed using an eight-noded quadrilateral element taking into account the stress concentration. The model was fixed in the right end and loaded with an axial stress $p = 10 \text{ MPa}$ at the left end.

The deformed shape and the von Mises stress distribution in the metal/composite overlapping area are presented in figures 2 and 3. It can be seen in Fig. 3 the singularities points at the end interfaces between the adhesive and the adherents. It was found that the distribution of stresses in the midplane of the glue layer does not depend on the FE meshing size of the adhesive area.

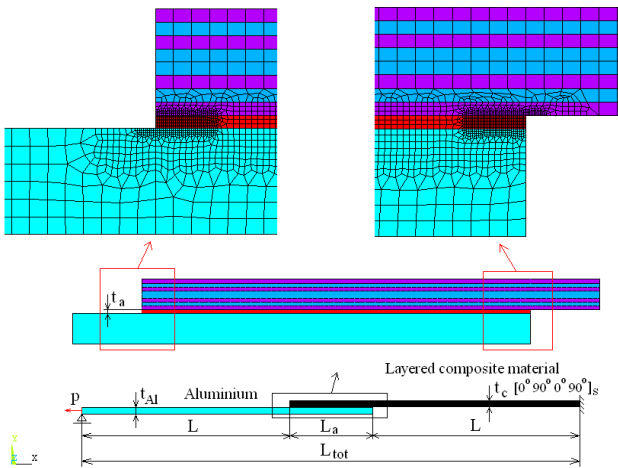


Fig. 1. 2D FE model

The 3D model (fig. 4) developed only on a half of the structure, due to the symmetry, was meshed with isotropic/layered 20 noded brick elements and was subjected to a similar tensile load, produced by a uniform $p = 10 \text{ MPa}$ pressure applied on the free

end. The deformed shape and the von Mises stress distribution, shown in figures 5 and 6, prove that the displacements are pretty much the same, but the maximum stresses, reached at the ends of the overlapping area are considerably lower, due to coarser meshing in this model.

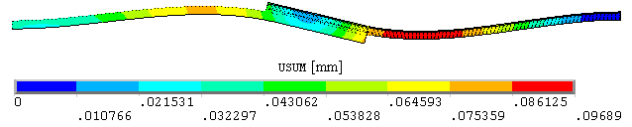


Fig. 2. Deformed shape of the virtual sample, 2D FE model (50 x total displacements - USUM)

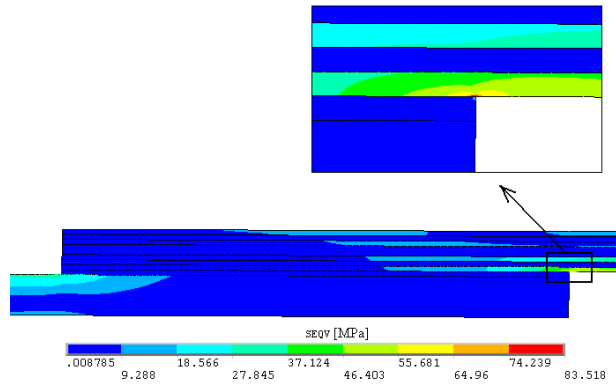


Fig. 3. Distribution of von Mises stresses in the overlapping area, 2D FE model

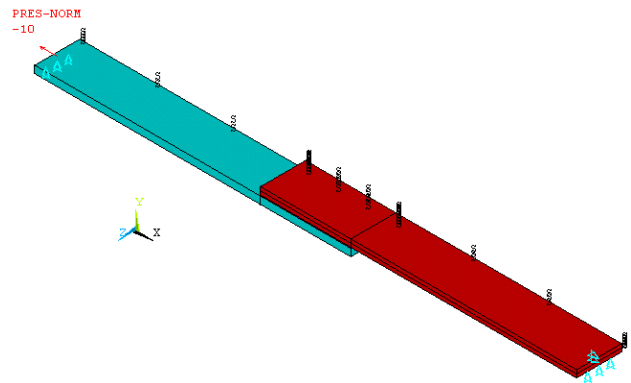


Fig. 4. 3D FE model. S denote symmetry boundary conditions and mesh is not shown

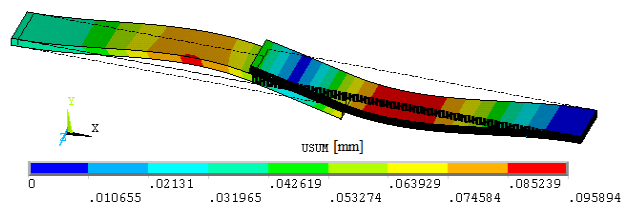


Fig. 5. Deformed shape of the virtual sample, 3D FE model (50 x total displacements - USUM)

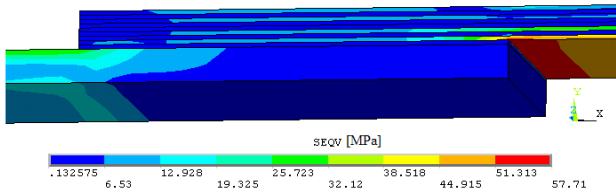


Fig. 6. Distribution of von Mises stresses in the overlapping area, 3D FE model.

2.2 Sensitivity Analysis

It is remarkable that the stress values in the midplane of the glue layer are quite close in the two models (see Fig. 7 and Fig. 8 for peeling stress distribution). For this reason, the 2D model was further used in evaluating the model sensitivity to various geometric and material parameters.

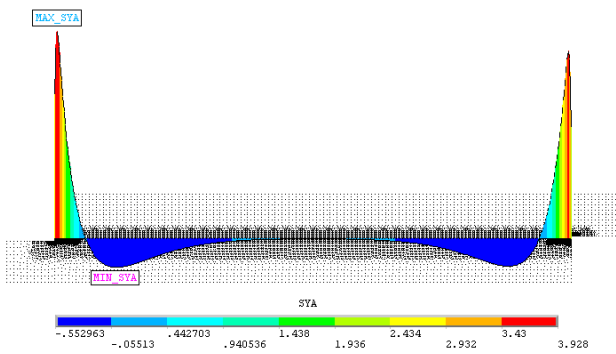


Fig. 7. Peeling stress (SY) distribution along the overlap area (length) in the middle plane of the adhesive from 2D model

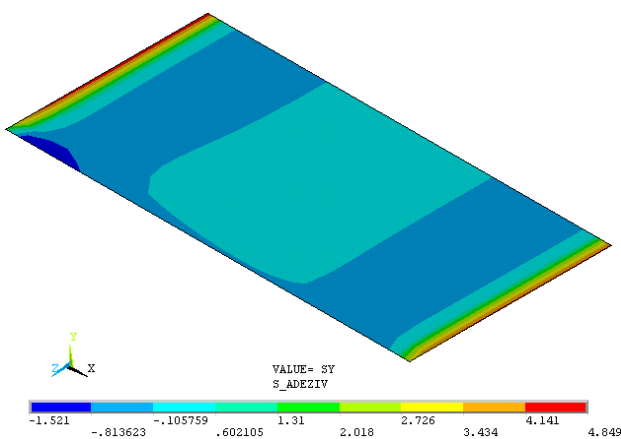


Fig. 8. Peeling stress (SY) distribution along the overlap area in the middle plane of the adhesive from 3D model

All the component stresses in the middle of the adhesive plane have maximum values in the vicinity of the ends length as can be shown in the figure 9.

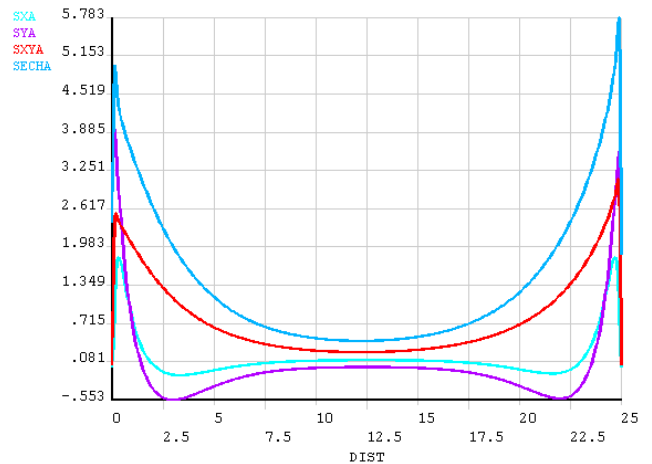


Fig. 9. Axial stress (SX), peeling stress (SY), shear stress (SXY) and von Mises (SECH) stress distribution along the overlap length in the middle plane of the adhesive from 2D model

In the sensitivity analysis the maximum and minimum values of the stresses (see Fig. 7) were monitored. For example, in figure 10 is presented the evolution of the extreme above mentioned stresses with the overlapping length (L_a). It is very clear that over 20 mm overlapping length the values of extreme stresses became quasi-constant.

In figure 11 is presented the evolution of the same mentioned stresses with the adhesive thickness (t_a). It is clear that over 0.15 mm adhesive thickness the values of extreme stresses became quasi-constant. Another interesting evolution of the same stresses can be followed in figure 12, this time the parameter being the Young modulus (E_{ad}) of the adhesive layer. The steady increase of von Mises (SECH), peeling (SYA) and shear (SXYA) stresses with E_{ad} has to be retained.

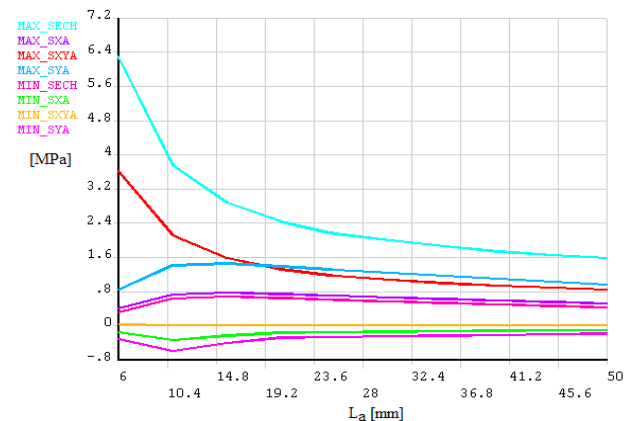


Fig. 10. Evolution of extreme stresses with overlapping distance

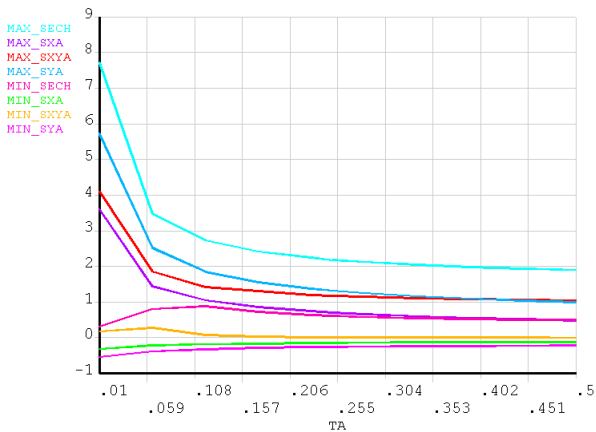


Fig. 11. Evolution of extreme stresses with adhesive thickness

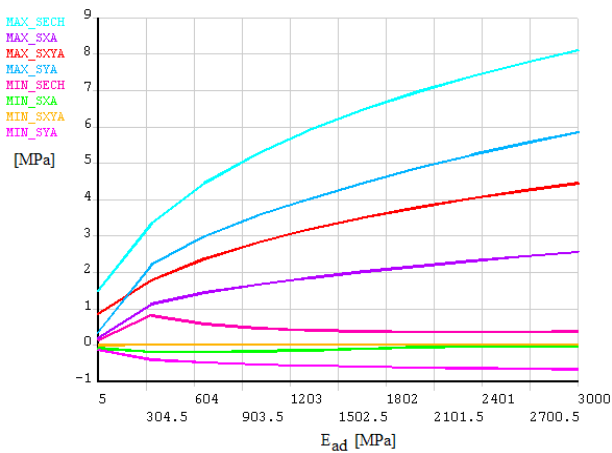


Fig. 12. Evolution of extreme stresses with Young modulus of the adhesive layer

If the Young modulus of the composite adherent is considered as a variable and all the remainder constants of the material are considered constants, for $E_{ad} = 100 \text{ MPa}$, the extreme stresses distribution are as in figure 13.

As some partial conclusions from linear static analysis we can say that: a) the maximum stresses in the adhesive decrease with the overlap length but for very short overlap lengths the adhesive is more uniform stressed as can be observed in figure 14; b) the maximum stresses in the adhesive decrease with the adhesive thickness and for very thick adhesive layers the adhesive is more uniform stressed as can be observed in figure 15; c) the maximum stresses in the adhesive increase with the Young's modulus of the adhesive, for very soft adhesive it is more uniform stressed as can be observed in figure 16; d) the maximum stresses in the adhesive decrease with the composite adherent stiffness (Young's modulus)

but these kind of study must supplementary investigated.

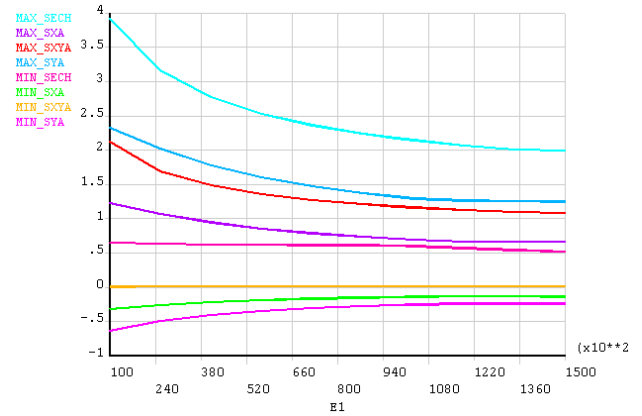


Fig. 13. Evolution of extreme stresses with principal Young modulus of the composite layer

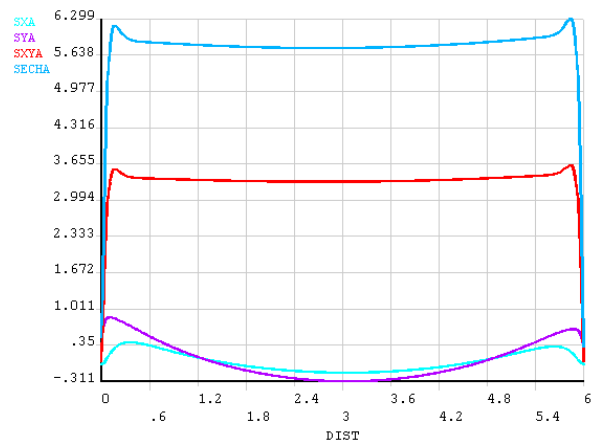


Fig. 14. Stresses distribution along the overlap length in the middle plane of the adhesive for $L_a = 6 \text{ mm}$

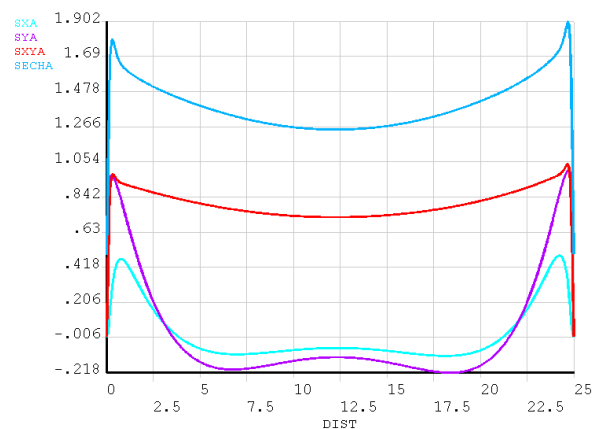


Fig. 15. Stresses distribution along the overlap length in the middle plane of the adhesive for $t_a = 0.5 \text{ mm}$

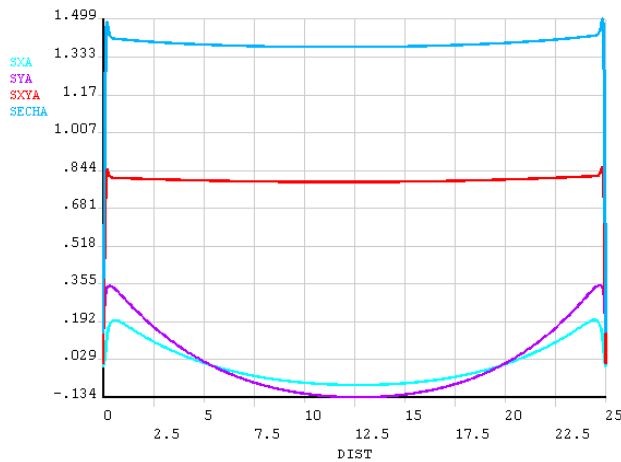


Fig. 16. Stresses distribution along the overlap length in the middle plane of the adhesive for $E_a = 5 \text{ MPa}$

3 Experimental results

The experiments were made on aluminum/composite lap joints with 12.5 mm and 25 mm average overlapping. The aluminum plate was always 1.6 mm thick, while the composites had variable thickness. The layered composites involved in the joints were GFRPs, with or epoxy resins, reinforced with satin type fabrics, made with prepreps or wet molding technology. The adhesives used were especially from the family of epoxy resins: AY103/HY991 and AW106/HV953.

The joints were subjected to tensile tests on a Tiratest 2200 universal testing machine which offered the possibility to load each member of the joint in its own plane. This was possible with the adjustable hydraulic grips of the machine, which can make the gripping of each end of a flat sample in a separate plane (fig. 17).

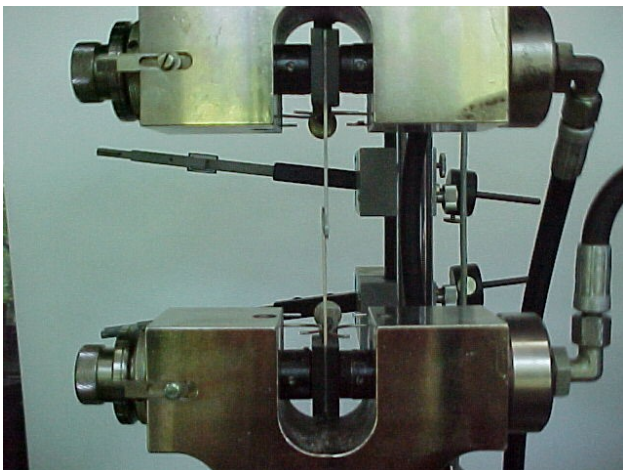


Fig. 17. Adjustable hydraulic gripping heads

Images of tested specimens are presented in figures 18-21. There are proofs for the best bonded interfaces, which failed leaving well balanced peeled surfaces on the two members of the lap joints, sometimes with some layer of the laminate left on the aluminum part. A quantitative view on the behavior of all lap joint can be followed in tables 1 and 2.



Fig. 18. Hybrid (aluminum/wet molded laminates, 6 layers) single lap joint aspect after static testing, for $L_a = 25 \text{ mm}$



Fig. 19. Hybrid (aluminum/wet molded laminates, 4 layers) single lap joint aspect after static testing, for $L_a = 25 \text{ mm}$

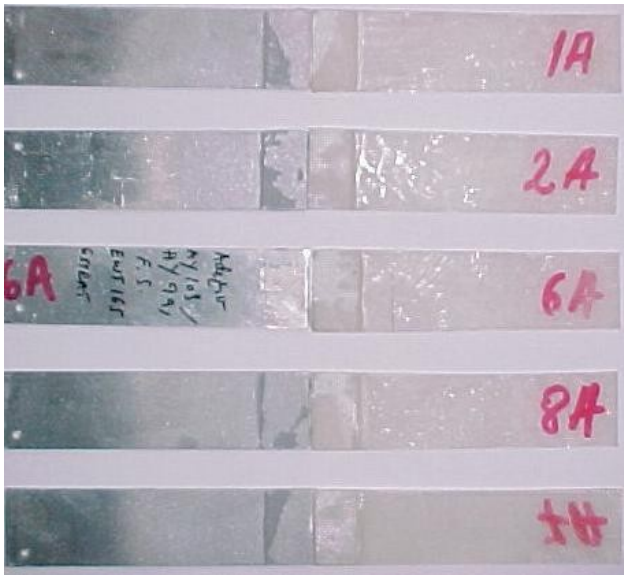


Fig. 20. Hybrid (aluminium/wet molded laminates, 6 layers) single lap joint aspect after static testing for $L_a = 12.5 \text{ mm}$



Fig. 20. Hybrid (aluminium/wet molded laminates, 4 layers) single lap joint aspect after static testing for $L_a = 12.5 \text{ mm}$

Table 2. Lap joints bonded with adhesive AY103/HY991

Composite member	Av. thick./ No. layers	Overlap. [mm]	F_{max} [N]
EWT 165 satin glass fiber fabric /polyester	0.8 mm/4	12.5	3387
		25	3877
	1.2 mm/6	12.5	3828
		25	5438
PREPREG satin glass fiber fabric /epoxy	1 mm/4	12.5	2606
		25	3192
	1.5 mm/6	12.5	2025
		25	3221

4 Discussion and Conclusions

The numerical analysis shows that 2D FE models provide rather similar results as more

complicated 3D models. For this reason, 2D models can be used for various analyses. The influence of the Young modulus of the glue in the stress state in the adhesive layer was completed with a study which proved that softer glues are the only ones to load the rivets in a mixed joint. Experiments proved that the decrease of extreme stress values for such glues has also to be considered for making an adequate choice of materials. There were also confirmed the sensitivities found by numerical analysis.

Table 3. Lap joints bonded with adhesive AW106/HV953

Composite member	Av.thick./ No. layers	Overlap. [mm]	F_{max} [N]
EWT 165 satin glass fiber fabric /epoxy	0.6 mm/3	12.5	3910
		25	4039
	1 mm/4	12.5	3907
		25	5098
PREPREG satin glass fiber fabric /epoxy	1 mm/4	12.5	4327
		25	5222
	0.25/6	12.5	3651
		25	4984

Acknowledgment: The research work and participation to ICCM-16 were financially supported by CEEEX projects COMPAS, DALEISC and SRMSSA, run under contracts with agencies of Romanian Ministry of Education and Research.

References

- [1] Baker A.A. and Jones R. "Bonded repair of aircraft structures". Martinus Nijhoff Publishers, Dordrecht, 1988.
- [2] Stewart M.L. "An Experimental Investigation of Composite Bonded and/or Bolted Repairs Using single Lap Joint Designs". *AIAA-97-1339*, pp 2752-2760, 1997.
- [3] Atre A.P., Johnson W.S. "Analysis of the effects of riveting process parameters on the fatigue of aircraft fuselage lap joints". *9th Joint FAA/DoD/NASA Aging Aircraft Conference, March 6-9, Hyatt Regency, Atlanta, GA, 2006.*
- [4] Belingardi G., Goglio L. Tarditi A. "Investigating the effect of spew and chamfer size on the stresses in metal/plastics adhesive joints", *International Journal of Adhesion & Adhesives*, 22, pp 273-282, 2002.
- [5] Caliskan M. "Evaluation of bonded and bolted repair techniques with finite element method". *Materials and Design*, 27, pp 811-820, 2006.
- [6] Kelly G. "Quasi-static strength and fatigue life of hybrid (bonded/bolted) composite single lap joints". *Composite structures*, 72, pp 119-129, 2006.